Supporting Information

Modeling of Human Hepatic and Gastrointestinal Ethanol Metabolism with Kinetic-Mechanism-Based Full-Rate Equations of the Component Alcohol Dehydrogenase Isozymes and Allozymes

Yu-Chou Chi,[†] Shou-Lun Lee,[‡] Yung-Ping Lee,[†] Ching-Long Lai,[§] and Shih-Jiun Yin[†]

[†]Department of Biochemistry, National Defense Medical Center, 161 Minchuan East Road Section 6, Taipei 11490, Taiwan
[‡]Department of Biological Science and Technology, China Medical University, 91 Hsueh-Shih Road, Taichung 40402, Taiwan
[§]Department of Nursing, Chang Gung University of Science and Technology, 261 Wenhwa First Road, Taoyuan City 33303, Taiwan

Corresponding Author
Shih-Jiun Yin, Department of Biochemistry, National Defense Medical Center, 161 Minchuan East Road Section 6, Taipei 11490, Taiwan.
E-mail: yinsj@ndmc.idv.tw. Tel: + 886 2 87923100 ext 18827. Fax: + 886 2 87923106

Contents of Supporting Information

(Continued)

steady-state rates than those with the *ADH1B*1* allele.

Table S6. Human hepatic and gastrointestinal mucosal ADH activities of different phenotypes.

Figure S1. Product inhibition patterns for human ADH isozymes and allozymes.

Figure S2. Dead-end inhibition patterns for human ADH isozymes and allozymes.

Figure S3. Reaction scheme of Ordered Sequential Bi Bi kinetic mechanism of human alcohol dehydrogenase.

Figure S4. Simulated ethanol saturation profile of human livers with different *ADH1B* and *ADH1C* genotypes.

Table S1. Protein Contents and Expression Pattern of ADH Isozymes in Human Liver and Gastrointestinal Mucosae

		Liver[a]		Stomach[a]		Duodenum[a]		Jejunum[a]		Tissue
Class	Isozyme	mg/g tissue	mg/organ	mg/g mucosa	mg/total mucosa	mg/g mucosa	mg/total mucosa	mg/g mucosa	mg/total mucosa	distribution[b]
I	ADH1A	1.9	2660							L
	ADH1B	5.8	8120							L
	ADH1C	1.9	2660	0.28	6.44	0.11	3.74	0.15	22.4	L, S, D, J
II	ADH2	1.65	2310			0.013	0.44	0.016	2.38	L, D, J
IV	ADH4			0.05	1.15					S

[a] Data for the protein contents of ADH isozymes in surgical human tissues (mg/g tissue) are from Chiang et al.,[12,14] Lee et al.,[18] and Yin et al.[13] The isozyme protein amounts in liver were ADH1 = 9.62 ± 0.52 mg/g tissue (range 7.22–12.79 mg/g tissue; n = 11) and ADH2 = 1.65 ± 0.12 mg/g tissue (1.22–2.42 mg/g tissue; n = 11);[12] in duodenal mucosa, ADH1 = 0.108 ± 0.015 mg/g tissue (0.068–0.175 mg/g tissue; n = 7) and ADH2 = 0.0125 ± 0.0029 mg/g tissue (0.0023–0.0224 mg/g tissue; n = 7);[14] in jejunal mucosa, ADH1 = 0.147 ± 0.015 mg/g tissue (0.080–0.196 mg/g tissue; n = 7) and ADH2 = 0.0159 ± 0.0047 mg/g tissue (0.0052–0.0407 mg/g tissue; n = 7).[14] The total protein contents of isozymes, i.e., mg/organ or mg/total mucosa, were calculated by multiplying the tissue masses of human liver and gastrointestinal mucosae (Lee et al.[18] and James et al.[41]).

[b] Data for liver (L), stomach (S), duodenum (D) and jejunum (J) taken from Chiang et al.[12,14] and Yin et al.[13]

Table S2. Maximum Ethanol-Oxidizing and Acetaldehyde-Reducing Velocities of ADH Isozymes and Allozymes in Human Liver and Gastrointestinal Mucosae

Class	Isozyme/allozyme	V_{max}	Isozyme/allozyme (μmol/min/mg protein)	Liver (mmol/min/organ)	Stomach (mmol/min/total mucosa)	Duodenum (mmol/min/total mucosa)	Jejunum (mmol/min/total mucosa)
I	ADH1A	V^{f}_{max}	0.55 ± 0.03	1.5			
		V^{r}_{max}	9.3 ± 0.2	25			
	ADH1B1	V^{f}_{max}	0.15 ± 0.01	1.2			
		V^{r}_{max}	6.5 ± 0.3	53			
	ADH1B2	V^{f}_{max}	7.5 ± 0.3	61			
		V^{r}_{max}	140 ± 10	1100			
	ADH1B3	V^{f}_{max}	10 ± 1	81			
		V^{r}_{max}	58 ± 3	470			
	ADH1C1	V^{f}_{max}	0.75 ± 0.03	2.0	0.0048	0.0028	0.017
		V^{r}_{max}	18 ± 1	48	0.12	0.067	0.40
	ADH1C2	V^{f}_{max}	0.48 ± 0.03	1.3	0.0031	0.0018	0.011
		V^{r}_{max}	11 ± 1	29	0.071	0.041	0.25
II	ADH2	V^{f}_{max}	0.20 ± 0.01	0.46		0.000088	0.00048
		V^{r}_{max}	6.5 ± 0.3	15		0.0029	0.015
IV	ADH4	V^{f}_{max}	22 ± 1		0.025		
		V^{r}_{max}	650 ± 30		0.75		

Distribution of ADH isozymes in tissues and the tissue isozyme protein contents are shown in Supporting Information Table S1, assuming that protein contents of the allozymes encoded by the corresponding polymorphic gene locus are identical. V^{f}_{max} and V^{r}_{max} are maximum ethanol-oxidizing and maximum acetaldehyde-reducing velocities, respectively. The equation of interconversion between V_{max} of ADH isozymes expressed as mmol/min per organ or total mucosa and that expressed as μmol/min per mg ADH isozyme is following:

(Continued)

V_{max} (mmol/min per organ or total mucosal tissue) = V_{max} (μmol/min per mg ADH isozyme) × (mg ADH isozyme per organ or total mucosal tissue) × 10^{-3}. For equation of interconversion between k_{cat} and V_{max} of the isozymes, see footnote *c* in Table 2.

Table S3. Composite Numerical Rate Equations for Steady-State Metabolism of Ethanol with Component ADH Isozymes and Allozymes in Human Livers of Different Genotypes

Isozyme/allozyme	Numerical rate equation[a]
ADH1A	$v = \frac{38AB - 120000PQ}{5.4 + 120A + 0.30B + 25AB + 24P + 13000Q + 4700PQ + 520AP + 740BQ + 29ABP + 43BPQ}$
ADH1B1	$v = \frac{64AB - 200000PQ}{0.052 + 0.69A + 0.58B + 53AB + 25P + 350Q + 3800PQ + 330AP + 3200BQ + 220ABP + 270BPQ}$
ADH1B2	$v = \frac{67000AB - 210000000PQ}{670 + 700A + 230B + 1100AB + 19000P + 77000Q + 190000PQ + 20000AP + 36000BQ + 2500ABP + 11000BPQ}$
ADH1B3	$v = \frac{38000AB - 120000000PQ}{28000 + 13000A + 400B + 470AB + 44000P + 540000Q + 260000PQ + 20000AP + 10000BQ + 160ABP + 1200BPQ}$
ADH1C1	$v = \frac{96AB - 300000PQ}{1.6 + 12A + 0.35B + 48AB + 210P + 1300Q + 6300PQ + 1600AP + 210BQ + 300ABP + 530BPQ}$
ADH1C2	$v = \frac{38AB - 120000PQ}{0.21 + 4.9A + 0.14B + 29AB + 19P + 860Q + 4100PQ + 450AP + 520BQ + 140ABP + 290BPQ}$
ADH2	$v = \frac{6.9AB - 22000PQ}{18 + 200A + 0.17B + 15AB + 28P + 28000Q + 1500PQ + 290AP + 230BQ + 2.7ABP + 1.6BPQ}$

Six combinatorial homozygous genotypes of *ADH1B* and *ADH1C* occur in human populations: *ADH1B*1/*1–ADH1C*1/*1* (individuals homozygous for the *ADH1B*1* and the *ADH1C*1* alleles), *ADH1B*1/*1–ADH1C*2/*2* (homozygous for both *ADH1B*1* and *ADH1C*2*), *ADH1B*2/*2–ADH1C*1/*1* (homozygous for both *ADH1B*2* and *ADH1C*1*), *ADH1B*2/*2–ADH1C*2/*2* (homozygous for both *ADH1B*2* and *ADH1C*2*), *ADH1B*3/*3–ADH1C*1/*1* (homozygous for both *ADH1B*3* and *ADH1C*1*), and *ADH1B*3/*3–ADH1C*2/*2* (homozygous

for both *ADH1B*3* and *ADH1C*2*). The complete steady-state kinetic equation (Eq. 6) of the component isozymes and allozymes was applied to constructing organ models. Composite steady-state rate equations of the *ADH1B*1/*1–ADH1C*1/*1* liver are linear combination of the numerical rate equations for the component isozymes and allozymes of ADH1A, ADH1B1, ADH1C1 and ADH2; those for the remaining genotypes can be constructed in the similar way. Variables *A*, *B*, *P*, and *Q* are steady-state concentrations of NAD^+, ethanol, acetaldehyde, and NADH, respectively. For Michaelis constants K_a, K_b, K_p, and K_q (expressed as mM) as well as for product inhibition constants K_{ia}, K_{ib}, K_{ip} and K_{iq} (as mM) of the corresponding isozymes and allozymes, see Table 2. For maximum velocities of ethanol oxidation (V^f_{max}) and acetaldehyde reduction (V^r_{max}) (expressed as mmol/min per organ) of the corresponding isozymes and allozymes, see Supporting Information Table S2. Equilibrium constant, $K_{eq} = 3.16 \times 10^{-4}$, was used in Eq. 6 as that in the absence of buffer H^+ (pH 7.5), i.e., 10×10^{-12} M ÷ $10^{-7.5}$ M = 3.16×10^{-4}.

[a] The units for variables (*A*, *B*, *P*, *Q*) and individual isozyme and allozyme steady-state activities (*v*) in the component rate equations are expressed as mM and mmol/min per liver, respectively.

Table S4. Composite Numerical Rate Equations for Steady-State Metabolism of Ethanol with Component ADH Isozymes and Allozymes in Human Gastrointestinal Mucosae of Different Genotypes

Organ	Isozyme/allozyme	Numerical rate equation[a]
Stomach	ADH1C1	$v = \frac{0.00058AB - 1.8PQ}{0.0041 + 0.031A + 0.00088B + 0.12AB + 0.50P + 3.2Q + 15PQ + 3.9AP + 0.52BQ + 0.75ABP + 1.3BPQ}$
	ADH1C2	$v = \frac{0.00022AB - 0.70PQ}{0.00051 + 0.012A + 0.00034B + 0.071AB + 0.045P + 2.1Q + 9.8PQ + 1.1AP + 1.3BQ + 0.34ABP + 0.70BPQ}$
	ADH4	$v = \frac{0.019AB - 59PQ}{15 + 24A + 0.11B + 0.75AB + 14P + 1900Q + 79PQ + 23AP + 14BQ + 0.033ABP + 0.14BPQ}$
Duodenum	ADH1C1	$v = \frac{0.00019AB - 0.59PQ}{0.0023 + 0.017A + 0.00049B + 0.067AB + 0.29P + 1.9Q + 8.9PQ + 2.2AP + 0.29BQ + 0.42ABP + 0.74BPQ}$
	ADH1C2	$v = \frac{0.000074AB - 0.23PQ}{0.00029 + 0.0070A + 0.00020B + 0.041AB + 0.026P + 1.2Q + 5.7PQ + 0.62AP + 0.73BQ + 0.20ABP + 0.41BPQ}$
	ADH2	$v = \frac{0.00000026AB - 0.00081PQ}{0.0035 + 0.038A + 0.000032B + 0.0029AB + 0.0053P + 5.3Q + 0.28PQ + 0.056AP + 0.044BQ + 0.00052ABP + 0.00031BPQ}$
Jejunum	ADH1C1	$v = \frac{0.0068AB - 22PQ}{0.014 + 0.10A + 0.0029B + 0.40AB + 1.8P + 11Q + 54PQ + 14AP + 1.7BQ + 2.5ABP + 4.5BPQ}$
	ADH1C2	$v = \frac{0.0028AB - 8.7PQ}{0.0018 + 0.043A + 0.0012B + 0.25AB + 0.16P + 7.3Q + 35PQ + 3.8AP + 4.4BQ + 1.2ABP + 2.5BPQ}$
	ADH2	$v = \frac{0.0000072AB - 0.023PQ}{0.018 + 0.20A + 0.00017B + 0.015AB + 0.029P + 29Q + 1.5PQ + 0.31AP + 0.23BQ + 0.0027ABP + 0.0017BPQ}$

The complete steady-state kinetic equation (Eq. 6) of the component isozymes and allozymes was applied to constructing tissue models. Composite steady-state rate equations of the homozygous *ADH1C*1/*1* and the homozygous *ADH1C*2/*2* gastric mucosae are linear combination of the numerical rate equations for ADH1C1 and ADH4, and for ADH1C2 and ADH4, respectively; those of the duodenum and jejunum with different genotypes can be constructed in the similar way with ADH1C allozymes and ADH2. For Michaelis constants and product inhibition constants of the corresponding isozymes and allozymes, see Table 2. For maximum velocities V_{max}^{f} and V_{max}^{r} of the corresponding isozymes and allozymes per total mucosal tissue, see Supporting Information Table S2. Variables *A*, *B*, *P*, and *Q* are steady-state concentrations of NAD^+, ethanol, acetaldehyde, and NADH, respectively. Equilibrium constant, $K_{eq} = 3.16 \times 10^{-4}$, which was described in Supporting Information Table S3.

[a] The units for variables (*A*, *B*, *P*, *Q*) and individual isozyme and allozyme activities (*v*) in the component rate equations are expressed as mM and mmol/min per total mucosa, respectively.

Table S5. Simulated Relative Contributions of the Component ADH Isozymes and Allozymes in Human Livers with *ADH1B*2* and *ADH1B*3* Alleles at 15% Higher Steady-State Rates Than Those With the *ADH1B*1* Allele

		Relative ethanol-metabolizing activity (%) at various ethanol concentrations (mM)				
Genotpe	Isozyme/Allozyme	1	2.5	5	10	25
*ADH1B*2/*2–ADH1C*1/*1*	ADH1A	1.1	1.6	2.2	2.8	3.5
	ADH1B2	93	94	94	94	93
	ADH1C1	6.0	4.7	3.9	3.2	2.3
	ADH2	0.11	0.20	0.32	0.53	0.99
*ADH1B*3/*3–ADH1C*1/*1*	ADH1A	—[a]	11	11	10	7.8
	ADH1B3	—[a]	40	58	72	84
	ADH1C1	—[a]	48	30	16	6.1
	ADH2	—[a]	1.3	1.4	1.8	2.1

For concentrations of NAD^+, acetaldehyde, and NADH at varied ethanol for the livers with genotypes *ADH1B*1/*1–ADH1C*1/*1*, *ADH1B*2/*2–ADH1C*1/*1*, and *ADH1B*3/*3–ADH1C*1/*1*, see Table 8. For simulated rates of *ADH1B*1/*1–ADH1C*1/*1* liver at the various ethanol concentrations, see Table 4. The simulated rates of livers carrying the *ADH1B*2* and the *ADH1B*3* alleles are 15% higher than those of the corresponding *ADH1B*1/*1* liver. The relative contributions of the component ADH isozymes and allozymes in simulated rates of *ADH1B*1/*1–ADH1C*1/*1* liver at the various ethanol concentrations are shown in Table 5.

[a] The steady-state rate of ADH1B*3/*3–*ADH1C*1/*1* liver at 1 μM acetaldehyde and 2 μM NADH is 17% lower than that of the *ADH1B*1/*1–ADH1C*1/*1* liver (Table 8 footnote).

Table S6. Human Hepatic and Gastrointestinal Mucosal ADH Activities of Different Phenotypes

			Activity	
Tissue	Phenotype	*n*	μmol/min/g tissue	μmol/min/total tissue
Liver	ADH1B*1/*1	15	2.32 ± 0.26	3250
	ADH1B*1/*2	55	10.9 ± 0.8	15300
	ADH1B*2/*2	71	13.9 ± 0.8	19500
Stomach	ADH1C*1/*1	169	0.238 ± 0.007	5.47
Duodenum	ADH1C*1/*1	91	0.357 ± 0.015	12.1
Jejunum	ADH1C*1/*1	23	0.293 ± 0.019	43.7

Data for surgical liver, stomach and duodenum/jejunum mucosal tissues are from Chiang et al.,[12] Yin et al.[13] and Chiang et al.,[14] respectively. The tissue homogenization and ultracentrifugation, phenotyping by isoelectric focusing, and activity assay were carried out according to the same protocols as described. ADH activities were determined in 0.1 M sodium phosphate, at pH 7.5 and 30 ℃, containing 33 mM ethanol, 2.4 mM NAD^+, and 1 mM semicarbazide. Values represent the mean ± SE. For estimated total masses of the tissues, see Supporting Information Table S1 footnote.

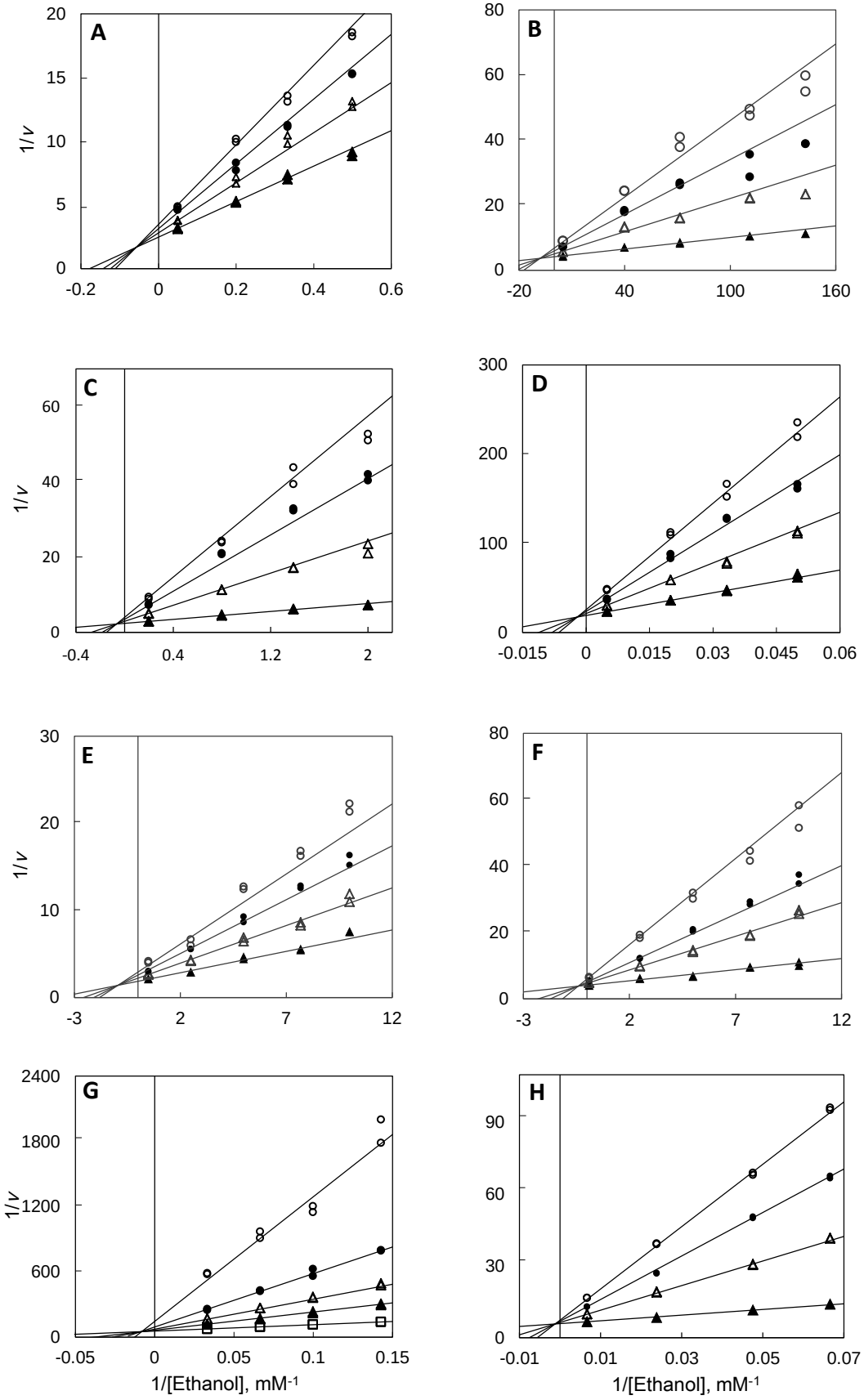

Figure S1. Product inhibition patterns for human ADH isozymes and allozymes. The buffer for kinetic studies was 0.1 M sodium phosphate at pH 7.5 and 25 °C. Concentrations of varied substrate are indicated on the graphs. Concentrations of the inhibitor increase from bottom to top. Velocities are expressed as ΔA_{340}/min for panels

(Continued)

D and *G*; and ΔF_{460}/min for panels *A*–*C*, *E*, *F*, and *H*. *A*, ADH1A, inhibition by 0, 0.15, 0.3, and 0.45 mM acetaldehyde at 0.1 mM NAD^+; 19 nN enzyme; K_{is} was 0.36 ± 0.03 mM, and K_{ii} was 1.1 ± 0.2 mM. *B*, ADH1B1, inhibition by 0, 0.05, 0.1, and 0.15 mM acetaldehyde at 2.4 mM NAD^+; 22 nN enzyme; K_{is} was 0.027 ± 0.002 mM, and K_{ii} was 0.24 ± 0.03 mM. *C*, ADH1B2, inhibition by 0, 0.1, 0.2, and 0.3 mM acetaldehyde at 2.4 mM NAD^+; 2.5 nN enzyme; K_{is} was 0.033 ± 0.002 mM, and K_{ii} was 0.47 ± 0.08 mM. *D*, ADH1B3, inhibition by 0, 4, 8, and 12 mM acetaldehyde at 2 mM NAD^+; 30 nN enzyme; K_{is} was 0.41 ± 0.02 mM, and K_{ii} was 4.2 ± 0.6 mM. *E*, ADH1C1, inhibition by 0, 0.03, 0.06, and 0.09 mM acetaldehyde at 2.4 mM NAD^+; 3.3 nN enzyme; K_{is} was 0.040 ± 0.004 mM, and K_{ii} was 0.16 ± 0.02 mM. *F*, ADH1C2, inhibition by 0, 0.03, 0.05, and 0.1 mM acetaldehyde at 2.4 mM NAD^+; 9.5 nN enzyme; K_{is} was 0.15 ± 0.01 mM, and K_{ii} was 0.21 ± 0.02 mM. *G*, ADH2, inhibition by 0, 1, 2, 4, and 10 mM acetaldehyde at 1.2 mM NAD^+; 400 nN enzyme; K_{is} was 0.55 ± 0.02 mM, and K_{ii} was 5.7 ± 1.0 mM. *H*, ADH4, inhibition by 0, 2.5, 5, and 7.5 mM acetaldehyde at 2.4 mM NAD^+; 1.4 nN enzyme; K_{is} was 0.78 ± 0.02 mM, and K_{ii} was 23 ± 3 mM. The normality of enzyme was calculated based on a subunit molecular mass of 40 kDa; nN is nanonormality, i.e., 10^{-9} normality.

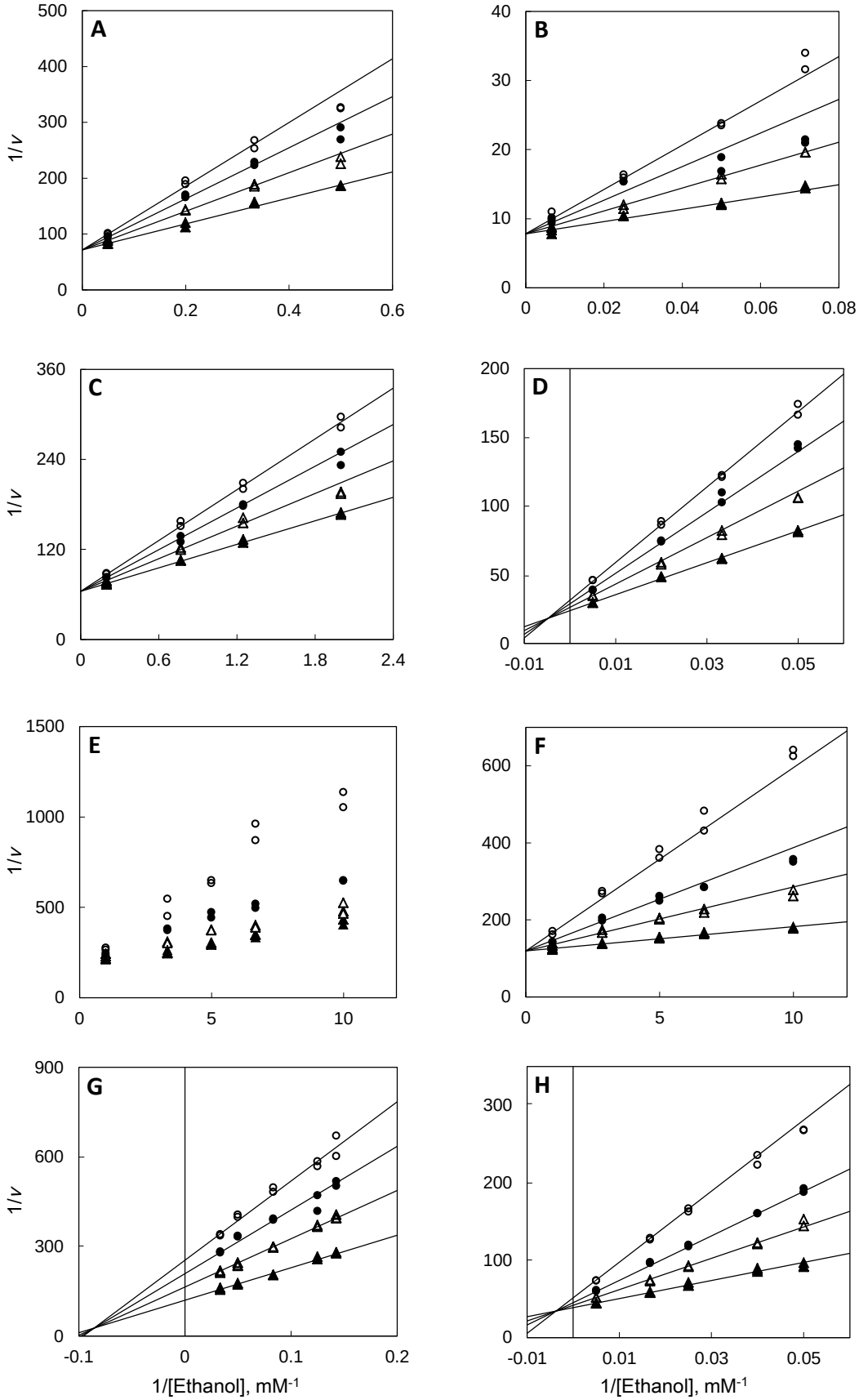

Figure S2. Dead-end inhibition patterns for human ADH isozymes and allozymes. The buffer for kinetic studies was 0.1 M sodium phosphate at pH 7.5 and 25 °C. Concentrations of varied substrate are indicated on the graphs. Concentrations of the inhibitor increase from bottom to top. Velocities are expressed as ΔA_{340}/min for panels

(Continued)

A and *C–H*; and ΔF_{460}/min for panel *B*. *A*, ADH1A, inhibition by 0, 0.5, 1, and 1.5 μM 4MP (4-methylpyrazole) at 2.4 mM NAD^+; 100 nN enzyme; K_{is} was 1.0 ± 0.1 μM. *B*, ADH1B1, inhibition by 0, 0.33, 0.66, and 0.99 μM 4MP at 2.4 mM NAD^+; 17 nN enzyme; K_{is} was 0.38 ± 0.04 μM. *C*, ADH1B2, inhibition by 0, 0.2, 0.4, and 0.6 μM 4MP at 2.4 mM NAD^+; 7.5 nN enzyme; K_{is} was 0.52 ± 0.02 μM. *D*, ADH1B3, inhibition by 0, 1.5, 3, and 4.5 μM 4MP at 2.4 mM NAD^+; 23 nN enzyme; K_{is} was 3.3 ± 0.2 μM, and K_{ii} was 14 ± 1 μM. *E*, ADH1C1, inhibition by 0, 0.05, 0.1, and 0.2 μM 4MP at 2.4 mM NAD^+; 22 nN enzyme; K_{is} was 0.069 ± 0.006 μM. *F*, ADH1C2, inhibition by 0, 0.1, 0.2, and 0.4 μM 4MP at 2.4 mM NAD^+; 32 nN enzyme; K_{is} was 0.061 ± 0.004 μM. *G*, ADH2, inhibition by 0, 0.5, 1, and 1.5 mM 4MP at 2.4 mM NAD^+; 59 nN enzyme; K_{is} was 1.0 ± 0.1 mM, and K_{ii} was 1.3 ± 0.1 mM. *H*, ADH4, inhibition by 0, 0.2, 0.4, and 0.8 mM 4MP at 2.4 mM NAD^+; 110 nN enzyme; K_{is} was 0.27 ± 0.01 mM, and K_{ii} was 2.4 ± 0.3 mM. The normality of enzyme was calculated based on a subunit molecular mass of 40 kDa; nN is nanonormality, i.e., 10^{-9} normality.

.

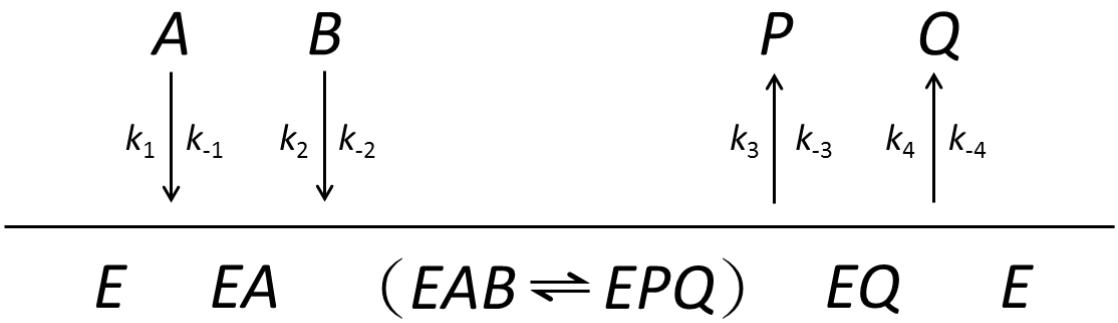

Figure S3. Reaction scheme of Ordered Sequential Bi Bi kinetic mechanism of human alcohol dehydrogenase isozymes and allozymes. *E*, enzyme; *A*, NAD^+; *B*, ethanol; *P*, acetaldehyde; *Q*, NADH.

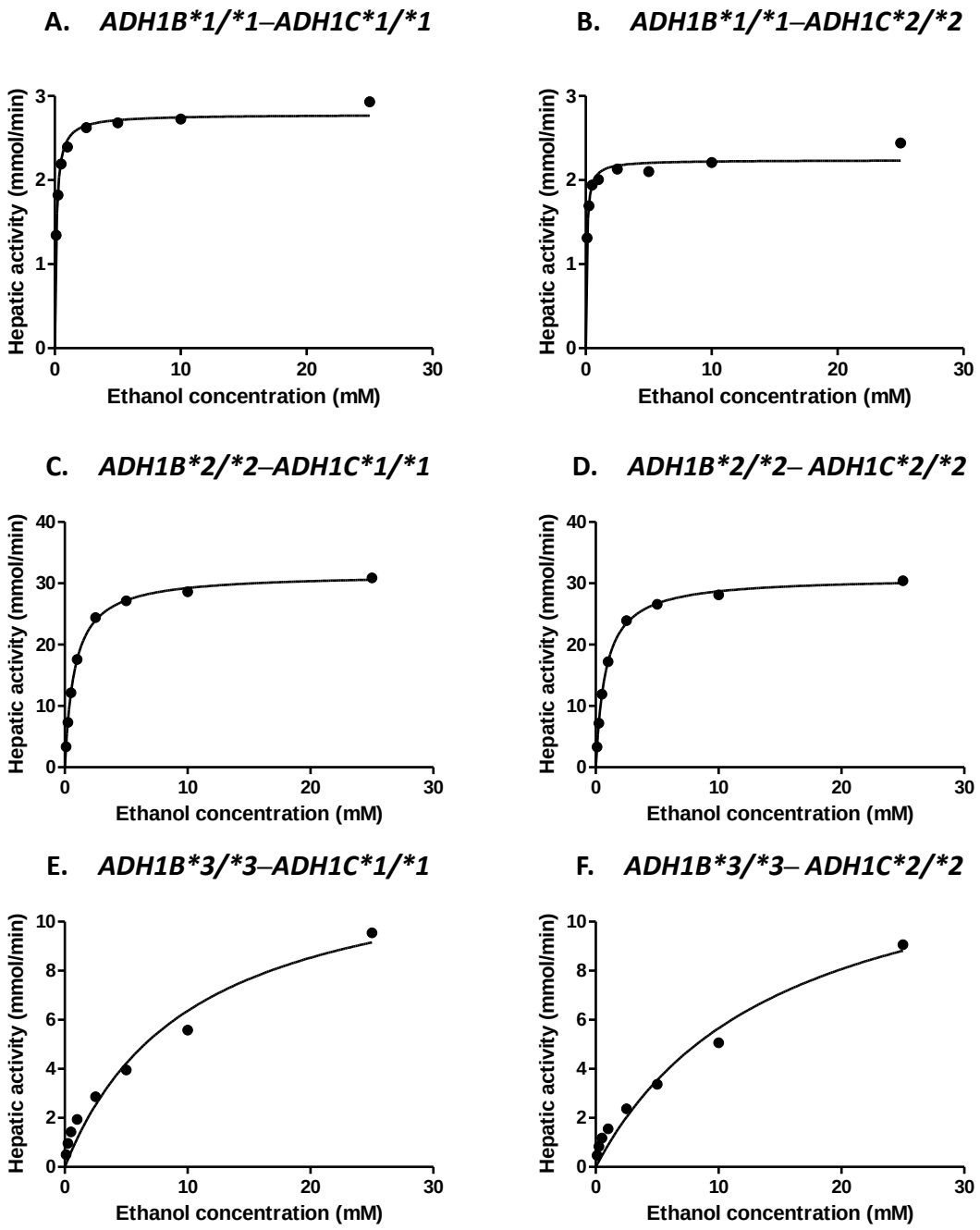

Figure S4. Simulated ethanol saturation profile of human livers with different *ADH1B* and *ADH1C* genotypes. Six combinationial genotypes of the homozygous *ADH1B*1/*1*, *ADH1B*2/*2* and *ADH1B*3/*3*, and the homozygous *ADH1C*1/*1* and *ADH1C*2/*2* are shown. For numerical rate equations of the component hepatic ADH isozymes and allozymes, see Supporting Information Table S3. Human liver is composed of ADH1A, ADH1B, ADH1C and ADH2 isozymes with allozymes ADH1B1, ADH1B2 or ADH1B3 and allozymes ADH1C1 or ADH1C2. The simulated hepatic steady-state ethanol-metabolizing activities were fit to Michaelis–Menten equation (Eq. 1) with HYPER program. For ethanol concentrations used and the corresponding concentrations of NAD^+, NADH and acetaldehyde in hepatocytes, see Table 6.